LETTERS

The purpose of this Letters section is to provide rapid dissemination of important new results in the fields regularly covered by Physics of Plasmas. Results of extended research should not be presented as a series of letters in place of comprehensive articles. Letters cannot exceed four printed pages in length, including space allowed for title, figures, tables, references and an abstract limited to about 100 words. ***There is a three-month time limit, from date of receipt to acceptance, for processing Letter manuscripts. Authors must also submit a brief statement justifying rapid publication in the Letters section.***

Transient ionization in plasmas produced by point-like irradiation of solid Al targets

L. A. Gizzi, C. A. Cecchetti, M. Galimberti,[a] A. Giulietti, D. Giulietti,[a] L. Labate,[b] S. Laville, and P. Tomassini
Intense Laser Irradiation Laboratory-IPCF, Area della Ricerca CNR, Via Moruzzi 1, 56124 Pisa, Italy

(Received 25 July 2003; accepted 15 September 2003)

Time-resolved x-ray spectroscopy has been used to investigate ionization dynamics of a micrometer-sized nanosecond laser-plasma during the plasma start-up phase. Experimental results are modeled using two-dimensional hydrodynamic simulations and time-dependent collisional-radiative calculations. The study clearly shows that, due to the rapid expansion cooling, x-ray emission originates predominantly from a well-localized plasma region characterized by rapidly evolving hydrodynamic conditions. In this region, ionization dynamics is found to depart substantially from the steady-state regime. The measurements provide clear evidence of this transient ionization regime showing good agreement with the time-dependent calculations. © *2003 American Institute of Physics.* [DOI: 10.1063/1.1624603]

Plasma formation by intense laser irradiation of solids provides a unique opportunity to investigate x-ray emission properties of dense plasmas in non-local thermodynamic equilibrium (NLTE). The kinetic behavior of these plasmas is strongly dependent upon the specific properties of ion and electron populations and the modeling of x-ray emission can be carried out using numerical codes. These plasmas are the subject of investigations in many fields of applied and fundamental research, from laser-plasma sources to x-ray lasers, from inertial confinement fusion to laboratory astrophysics. On the other hand, x-ray emission from these plasmas can be used for benchmarking of kinetic codes,[1] provided plasma hydrodynamic properties are known in detail.

More recently, dedicated experiments have been performed for fundamental studies in atomic physics and hydrodynamics.[2,3] In these experiments, test plasmas are produced under controlled laser irradiation conditions to minimize uncertainties on the knowledge of plasma parameters. Plasmas are typically produced using picosecond or nanosecond laser pulses focused on the surface of a solid target[4] or using exploding foils.[5,6] Test plasmas are usually characterized using standard laser-plasma diagnostic techniques[7,8] and modeled with hydrodynamic codes, such as MEDUSA,[9,10] and non-LTE atomic physics calculations.[11]

Regardless of the test plasma configuration used, recent experiments[2,3] consistently suggest that even in plasmas dominated by a planar expansion, two- or three-dimensional hydrodynamic effects at the plasma boundaries may play a significant role when attempting to model the x-ray emission properties. Furthermore, the role of hydrodynamics becomes critical in the transient regimes of plasma formation, when x-ray emission takes place from plasma regions characterized by rapid changes and strong spatial gradients of hydrodynamic quantities.[12] In these circumstances the modeling of x-ray spectra requires fully time-dependent atomic-physics and multi-dimensional hydrodynamics with radiative transfer calculations.

In this letter we focus our interest on early stage plasma formation by laser irradiation of solid targets, i.e., on the plasma evolution at times comparable to the relaxation times of the ionization of the target starting from the cold material. We show the results of an experiment in which ionization of an Al plasma was investigated through time-resolved x-ray spectroscopy. Our measurements clearly show that during this interaction stage, a condition is obtained in which changes in hydrodynamic parameters of the x-ray emitting plasma occur on a timescale faster than the timescale of ionization.

A simple picture of the underlying physical scenario can be obtained considering an ionic system for which the time constant $\tau_{Z\to Z+1}$ for ionization from the charge stage Z to the charge stage $Z+1$ can be evaluated as $\tau_{Z\to Z+1}=N_{Z+1}/|dN_{Z+1}/dt|$ with

[a]Also at: Dipartimento di Fisica, Università di Pisa and INFM, Pisa, Italy.
[b]Also at: Dipartimento di Fisica, Università di Bologna, Bologna, Italy.

$$\frac{dN_{Z+1}}{dt} = n_e[(S_c^Z + S_R^Z)N_Z - (\alpha_{3B}^{Z+1} + \alpha_{RR}^{Z+1})N_{Z+1}]. \quad (1)$$

Here n_e is the plasma electron density, N_Z is the population of the charge state Z, S_c^Z and S_R^Z are the rates of collisional and photo-ionization from the charge state Z, respectively, while α_{3b}^{Z+1} and α_{RR}^{Z+1} are the rates of three-body and radiative recombination from the charge state $Z+1$.

From the equations above the value of $\tau_{Z\to Z+1}$ has been estimated[13] for an optically thin Al plasma (neglecting S_R) at an electron density of 10^{21} cm^{-3} (close to the critical density for 1 μm wavelength laser light) and for electron temperatures up to 1 keV, using analytical expressions[14] for S_c, α_{3b}, and α_{RR}. According to these calculations, the time $\tau_{\mathrm{Al}}(\mathrm{Li}\to\mathrm{He})$, i.e., the time to reach the He-like stage, starting from the Li-like stage, is much less than 100 ps for temperatures greater than 200 eV. In contrast, $\tau_{\mathrm{Al}}(\mathrm{He}\to\mathrm{H})$ is of the order of 100 ps at 400 eV and depends weakly upon the temperature. Since this value of the relaxation time is comparable with the rise-time of a nanosecond laser pulse, it is expected to come into play during early stage plasma ionization.

A detailed quantitative description requires complex numerical codes to predict the evolution of the plasma hydrodynamics and atomic physics. This Letter deals with this problem providing unambiguous spectroscopic evidence of transient ionization in nanosecond laser-produced plasmas.

The experiment was carried out at the Intense Laser Irradiation Laboratory using a 3 ns, 1.053 μm Nd:YLF single-mode (both longitudinal and transverse) laser.[15] The laser pulse was tight-focused on a polished, rotating cylindrical Al target using an f/4 optics. The intensity distribution in the focal spot was Gaussian with a 6 μm FWHM (full width at half maximum) and a Rayleigh length of about 100 μm, for a nominal maximum intensity on target of 10^{15} W/cm^2. The use of a single-mode laser pulse ensured that a diffraction-limited focal spot could be obtained whose intensity distribution (spatial and temporal) was well-known, temporally smooth, and reproducible from shot to shot. These circumstances enabled us to generate a highly reproducible plasma.[16]

We stress that in our point-like irradiation scheme, the diameter of the laser focal spot is much smaller than the expected longitudinal density scale-length of the plasma at the peak of the laser pulse. Under such conditions, due to the predominantly spherical expansion geometry, a rapid cooling of the coronal region takes place giving rise to a highly inhomogeneous longitudinal temperature profile throughout the plasma. As discussed below, these circumstances have general[17,18] important consequences on the x-ray emission properties of our plasmas.[16,19,20]

We carried out ps-resolution x-ray spectroscopy to investigate *K*-shell emission from the He-like and H-like Al during the rise time of the laser pulse. X-ray spectra were acquired using a time-resolving crystal spectrometer mounted on the horizontal plane at 45° from the plasma expansion axis. The spectrometer was equipped with a flat thallium hydrogen phthalate TlAP crystal ($2d = 25.9$ Å) mounted in the first order Bragg configuration to spectrally resolve x-ray emission from approximately 6 to 8 Å. The spectrum was

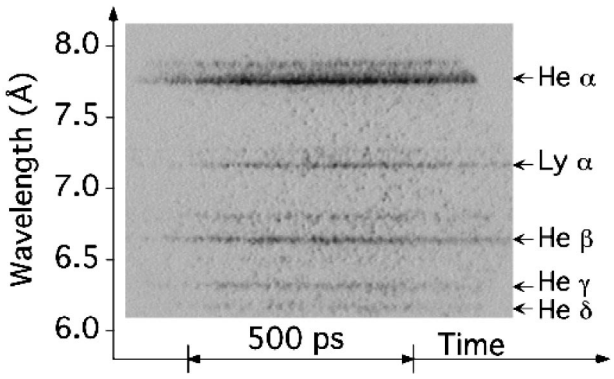

FIG. 1. Typical raw time-resolved x-ray spectrum of early *K*-shell emission from Al plasma observed at 45° from the plasma expansion axis. The resonance series of He-like ions and the main resonance line of hydrogenic ions including the corresponding satellites are clearly visible.

then time-resolved using a Kentech x-ray streak-camera fitted with a CsI photocathode and a 1 mm slit. The output phosphor screen of the streak-camera was imaged out using a CCD (charge coupled device) camera coupled to a digital image grabber.

We used an original experimental method[19] that enabled us to minimize the uncertainty in the relative intensity calibration of our time-resolved x-ray spectra. We cross-calibrated our time-resolving spectrometer against another x-ray spectrometer set to look simultaneously at the same plasma along an equivalent direction, i.e., symmetric with respect to the plasma expansion axis. This reference spectrometer was equipped with an x-ray sensitive, cooled CCD camera that allowed us to record intensity calibrated time-integrated spectra.[21] Spectra obtained with the streak-camera running in dc mode at different dc bias voltages were cross-calibrated against the CCD ones.

A typical, raw time-resolved x-ray spectrum of *K*-shell emission from the Al plasma, corrected for the geometrical streak-camera distortion, is shown in Fig 1. The temporal resolution, estimated taking into account the streak-rate and the signal-to-noise ratio, was found to be about 20 ps. The resonance series of He-like ions and the main resonance line of hydrogen-like ions including the corresponding satellites are clearly visible.

The general approach in the interpretation of spectra like the one shown in Fig. 1 is to model x-ray emission at selected He-like and H-like transition wavelengths for both steady-state (SS) and time-dependent (TD) conditions and then to compare the calculated ratios with the corresponding experimental ones. From an experimental viewpoint the best choice for the He-like emission is the He-β line while, concerning H-like transitions, signal-to-noise considerations led us to use the Ly-α resonance line. As we will discuss below, great care has been taken to evaluate opacity effects that are potentially important for these resonance lines.

We performed detailed hydrodynamic numerical simulations of our plasma using the two-dimensional (2-D) Eulerian hydro-code POLLUX.[22] The code includes laser absorption via inverse bremsstrahlung and thermal electron transport via flux-limited Spitzer–Harm conductivity. The plasma is supposed to be fully ionized and a perfect gas

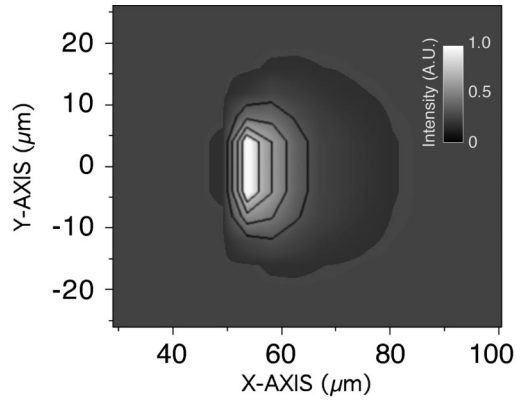

FIG. 2. Contour plot of the x-ray emission at the Ly-α wavelength taken 800 ps before the peak of the laser pulse. The emission was calculated using the code FLY to post-process POLLUX hydro-code results. Contour levels range from 0.2 (outer contour) to 0.8 (a.u.) and the maximum value of the emission is 1.

equation of state is used for electrons. We calculated the x-ray emission history by post-processing POLLUX results with the code suite FLY,[23] a time-dependent single-cell, collisional-radiative model for evaluation of *K*-shell emission from H-like through Be-like ions.

In general, simulations show that the instantaneous longitudinal x-ray emission profile calculated at the two transition wavelengths at different times during the laser pulse exhibits a very narrow peak, sitting on a long tail due to the plume of the plasma. The location of the peak moves inwards by approximately 10 μm during the entire laser pulse. Figure 2 shows the 2-D contour plot of the Ly-α emission intensity calculated at 800 ps before the peak of the 3 ns laser pulse. This plot shows indeed that most of the x-ray emission originates from a 3-μm-wide (FWHM) plasma slab close to the target surface (at $x=50$ μm), where a nearly planar expansion takes place. A much similar result with a slightly smaller longitudinal width is found for the He-β line.

According to these results we can therefore conclude that, despite the overall plasma hydrodynamic behavior, dominated by 2-D effects, the x-ray emission has a substantial one-dimensional (1-D) behavior. We can therefore restrict our further analysis to the 1-D longitudinal (along the target normal) profile.

Opacity effects were evaluated using the code FLY that takes into account reabsorption in an homogeneous plasma slab through the escape factors. The slab thickness was taken from the width (taken at a range of values with respect to the maximum) of the longitudinal profile of the corresponding ground state populations as retrieved by post-processing POLLUX simulations using FLY. By comparing line ratio calculated in this way with the experimental ratio at late times, when steady-state and time-dependent modeling give identical results, we found agreement when the width of the slab to be used in the simulation was the smallest possible. In other words, we can conclude that both the Ly-α and He-β lines are optically thin in our conditions. This gives us confidence that the Ly-α and He-β emission lines are reliable diagnostic lines for the evaluation of ionization dynamics in our plasma.

An important consequence of the above results is that, despite the largely inhomogeneous profile of our plasma during the start up phase, x-ray emission can be attributed to a layer of plasma with well-defined electron temperature and density. Therefore, we can attempt modeling our spectra using the values of the electron density and temperature at the position of the slab, i.e., where the calculated x-ray emission is maximum. The history of our reference temperature and density are given in Fig. 3.

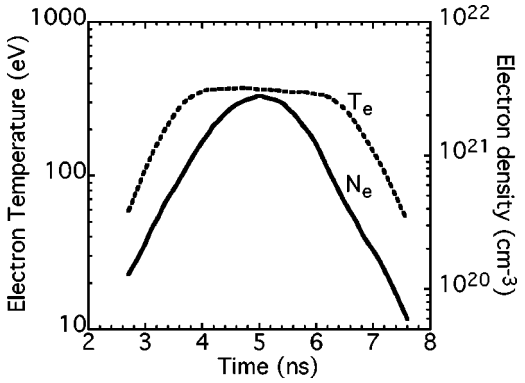

FIG. 3. History of electron temperature and density predicted by the 2-D code POLLUX for the plasma slab where x-ray emission is maximum. The peak of the laser pulse is located at 5 ns.

According to these plots, the electron temperature increases rapidly during the rise time of the pulse and reaches a plateau at approximately 400 eV. The plateau lasts approximately 2 ns, a duration significantly shorter than the FWHM of the laser pulse. In contrast, the electron density increases up to 3×10^{21} cm^{-3} at the peak of the laser pulse and decreases rapidly as the laser intensity decreases, having a value of approximately 4×10^{20} cm^{-3} 1.5 ns after the peak of the laser pulse.

We can now calculate the expected Ly-α to He-β intensity ratio processing the temperature and density history of Fig. 3 with the code FLY in both TD and SS conditions. The results of these calculations are shown in Fig. 4 for a time interval of 1.5 ns before the peak of the laser pulse located at 5 ns.

According to this plot, TD calculations (diamonds) differ from the SS ones (squares) during the rise of the laser pulse showing a Ly-α to He-β intensity ratio smaller than in the case of the SS calculation. This result is fully consistent with

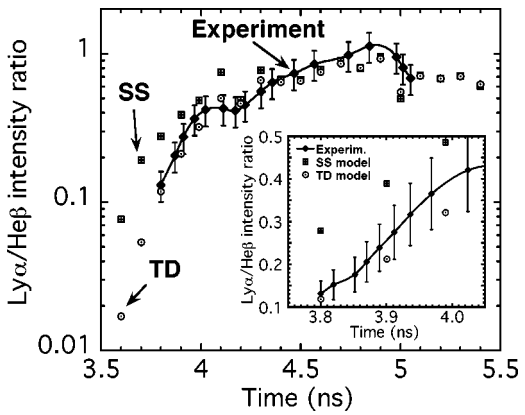

FIG. 4. Temporal evolution of the Ly-α to He-β intensity ratio (solid line) as obtained from the time resolved spectrum of Fig. 1. The experimental ratio (diamonds and interpolating curve) is compared to the intensity ratio calculated assuming a steady-state (square) or a time-dependent (circle) model.

the above-mentioned calculations obtained from Eq. (1). The difference between SS and TD calculated ratio decreases with time and the two calculations give identical results later than $t=4$ ns, i.e., 1 ns before the peak of the pulse.

The history of the Ly-α to He-β intensity ratio as measured from the time-resolved spectrum of Fig. 1 is also shown in Fig. 4. The time-axis of the calculated ratio is taken from the hydrodynamic simulations, while the temporal correlation with the experimental ratio was set minimizing the quadratic difference from the calculated ratio. This comparison immediately shows that, during the rise of the laser pulse, our experimental Ly-α to He-β intensity ratio is consistent only with the TD calculation, the SS calculations being completely outside the vertical error bars.

On the other hand, later in time, when the two models give identical results, our measurements agree with the calculated ratio. This is a very important point as it provides a test of reliability of our modeling, regardless of the specific issue of the identification of time-dependent effects.

It should be pointed out that the difference between the results of the two models would be hardly detected in time-integrated spectroscopic measurements. In fact, the total x-ray emission occurring during this start-up phase is negligible compared with the total emission during the entire laser pulse. Consequently, calculations and measurements of time-integrated intensity ratios would show no difference between the TD and the SS case.

On the other hand, the possibility of detecting this effect during the plasma start-up phase relies upon a smooth spatial and temporal evolution of the laser pulse. This work shows that such experimental conditions can be achieved using a simple point-like irradiation of a solid target with a temporally smooth laser pulse and accurate time-resolving spectroscopy.

In summary, a micrometer-sized test plasma has been produced by point-like irradiation of a solid target with a nanosecond laser pulse. Time-resolved spectroscopy of K-shell Al emission has been carried out during the plasma start-up phase and modeled using a 2-D hydrodynamic code and post-processing the data with a time-dependent NLTE atomic physics code. Calculations show a highly localized x-ray emission in a narrow planar slab near the critical density layer. characterized by rapidly changing hydrodynamic conditions. According to our time-dependent calculations, the ionization dynamics in this region during the plasma start-up phase exhibits a substantial deviation from the steady-state solutions. After a few hundreds of picoseconds, steady-state and time-dependent calculations give the same result. The Ly-α to He-β intensity ratio measured in our experiment during the plasma start-up phase enables us to discriminate between the two models being in a good agreement with the time-dependent calculations only.

ACKNOWLEDGMENTS

We would like to thank A. Barbini, A. Rossi, A. Salvetti, W. Baldeschi, and M. Voliani for their invaluable technical assistance.

S.L. acknowledges financial support from the European Research Training Network XPOSE Contract No. HPRN-CT-2000-00160. L.L. and P.T. acknowledge financial support from MIUR (Project ''Metodologie e diagnostiche per materiali ed ambiente''). This work was partially supported by the MIUR Project ''Impianti innovativi multiscopo per la produzione di radiazione X.''

[1] S.H. Glenzer, K.G. Estabrook, R.W. Lee, B.J. MacGowan, and W. Rozmus, J. Quant. Spectrosc. Radiat. Transf. **65**, 253 (2000).
[2] D.M. Chambers, P.A. Pinto, J. Hawreliak *et al.*, Phys. Rev. E **66**, 026410 (2002).
[3] M. Fajardo, P. Audebert, P. Renaudin, H. Yashiro, R. Shepherd, J.C. Gauthier, and C. Chenais-Popovics, Phys. Rev. Lett. **86**, 1231 (2001).
[4] L.A. Gizzi, A. Giulietti, O. Willi, and D. Riley, Phys. Rev. E **62**, 2721 (2000).
[5] O. Renner, J. Limpouch, E. Krousky, I. Uschmann, and E. Förster, J. Quant. Spectrosc. Radiat. Transf. **81**, 385 (2003).
[6] D.H. Phillion, E.M. Campbell, K.G. Estabrook, G.E. Phillips, and F. Ze, Phys. Rev. Lett. **49**, 1405 (1982).
[7] M. Borghesi, A. Giulietti, D. Giulietti, L.A. Gizzi, A. Macchi, and O. Willi, Phys. Rev. E **54**, 6769 (1996).
[8] L.A. Gizzi, D. Giulietti, A. Giulietti, T. Afshar-Rad, V. Biancalana, P. Chessa, E. Schifano, S.M. Viana, and O. Willi, Phys. Rev. E **49**, 5628 (1994).
[9] J.P. Christiansen, D.E.T.F. Ashby, and K.V. Roberts, Comput. Phys. Commun. **7**, 271 (1973).
[10] A. Djaoui and S.J. Rose, J. Phys. B **25**, 2745 (1992).
[11] P.K. Patel, J.S. Wark, D.J. Heading, A. Djiaoui, S.J. Rose, O. Renner, and A. Hauer, J. Quant. Spectrosc. Radiat. Transf. **57**, 683 (1997).
[12] W. Brunner and R.W. John, Laser Part. Beams **9**, 817 (1991).
[13] L.A. Gizzi, Ph.D. thesis, Imperial College of Science, Technology and Medicine, University of London, 1994.
[14] W. Lotz, Z. Phys. **220**, 486 (1969).
[15] D.C. Hanna and Y.-W.J. Koo, Opt. Commun. **43**, 414 (1982).
[16] L. Labate, M. Galimberti, A. Giulietti, D. Giulietti, L.A. Gizzi, and R. Numico, Laser Part. Beams **20**, 223 (2002).
[17] A. Rubenchick and S. Witkowsky, *Handbook of Plasma Physics* (North-Holland, Amsterdam, 1991), pp. 575–611.
[18] D. Giulietti and L.A. Gizzi, Riv. Nuovo Cimento **21**, 1 (1998).
[19] C.A. Cecchetti, M. Galimberti, A. Giulietti, L.A. Gizzi, L. Labate, and A. Salvetti (unpublished).
[20] L. Labate, A. Giulietti, D. Giulietti, L.A. Gizzi, R. Numico, and A. Salvetti, Laser Part. Beams **19**, 117 (2001).
[21] L. Labate, M. Galimberti, A. Giulietti, D. Giulietti, L.A. Gizzi, P. Tomassini, and G. Di Cocco, Nucl. Instrum. Methods Phys. Res. A **495**, 148 (2002).
[22] J. Pert, J. Comput. Phys. **43**, 111 (1981).
[23] R.W. Lee and T.J. Larsen, J. Quant. Spectrosc. Radiat. Transf. **56**, 535 (1996).